



Innovative Wind Energy System Featuring ANN-Controlled Pitch Regulation for Efficient Grid Integration

Tappeta Amar Kiran^{1*} , Dondapati Ravi Kishore² , Appana Naga Pavani¹, Baswa Uma Maheswari¹, Chappa Sravani Kumari¹

¹Department of Electrical and Electronics Engineering, Godavari Institute of Engineering and Technology (A), Rajahmundry.

²Department of Electrical and Electronics Engineering, Godavari Global University, Rajahmundry.

ABSTRACT: WECS are dynamic and intricate, considered by uncertainties and external disturbances. This research introduces an innovative pitch control strategy designed to improve energy stabilization and extraction predominantly for WT affected by unmodeled system dynamics to ensure stable operation under high wind speeds. For optimizing power capture, the ANN controller adapts dynamically to changing wind conditions by regulating the turbine blade's pitch angle. For grid integration, a PWM rectifier transforms the variable-frequency AC power from the turbine into DC power. The simulations are conducted in MATLAB/Simulink tool to evaluate the control framework. It reveals that the superior performance of the ANN controller in reducing mechanical loads on turbines and platforms maximizes power generation. Thus, it achieves reduced power and speed fluctuations, minimal overshoot, and enhances the dynamic behaviour of WT.

Review History:

Received: Jul. 17, 2025

Revised: Non. 22, 2025

Accepted: Mar. 09, 2026

Available Online: Jul. 01, 2026

Keywords:

VSI

WECS

DFIG

Pitch Control by ANN

PWM Rectifier

1- Introduction

Due to the rapid urbanization and population expansion, the global demand for energy has surged. The primary energy source is Fossil fuels. Due to the depletion of fossil fuel reserves, many countries face challenges in bridging the gap between energy supply and demand [1]. Moreover, the wide use of fossil fuels has harmful environmental impacts, including contributing to the greenhouse effect. There is a need for new energy sources to meet the ever-increasing need for energy while reducing the adverse effects on the environment [2-5]. Electricity generation from a variety of Renewable Energy Sources (RESs) has garnered a lot of attention in recent years [6]. In particular, wind power is one of the most promising forms in the global energy industry and is anticipated to continue growing quickly over the coming years [7-10]. Control systems need to be incorporated to guarantee the proper wind turbines (WT) operation and efficient utilization of wind energy to optimize power generation output, given the intricacy of wind energy systems and their significant reliance on climatic and environmental conditions. From a control perspective, a key goal is ensuring that the WT's output power remains near its rated level [11]. This is accomplished while minimizing fatigue and vibrations and optimizing efficiency. WT control systems aim to enhance

energy production, minimize mechanical loads, stabilize grid integration, and deliver uninterrupted power to the grid. To attain the specified control objectives, optimal control of blade pitch angle and generator torque is essential [12, 13]. The pitch manages the blade's rotation that regulates the wind's angle of attack to maximize the amount of available wind energy. Pitch control is a leading strategy for boosting power production in medium to large-sized wind turbines among various techniques. The pitch controller focuses on minimizing drag and increasing blade lift within the full-load operational range [14-16]. Fixed pitch stall control and variable pitch control represent two fundamental regulation methods for wind turbines. Variable pitch control maintains rotor speed stability by adjusting the blade pitch angle to match wind speed changes. Unfortunately, the frequent adjustments associated with this method can lead to increased blade stress and pitch servo fatigue, ultimately reducing turbine lifespan [17-18]. The majority of wind turbines currently use Proportional-Integral (PI) controllers because they are straightforward and simple to set up [19]. They efficiently control the rotor speed, guaranteeing maximum power production even under variable wind conditions. However, PI controllers overestimate blade pitch corrections in windy conditions, which results in instability and higher mechanical stress. By taking into consideration proportional, integral, and derivative actions, the PID controller, which is developed in [20], provides precise control and guarantees steady

*Corresponding author's email: amarkiran@giet.ac.in



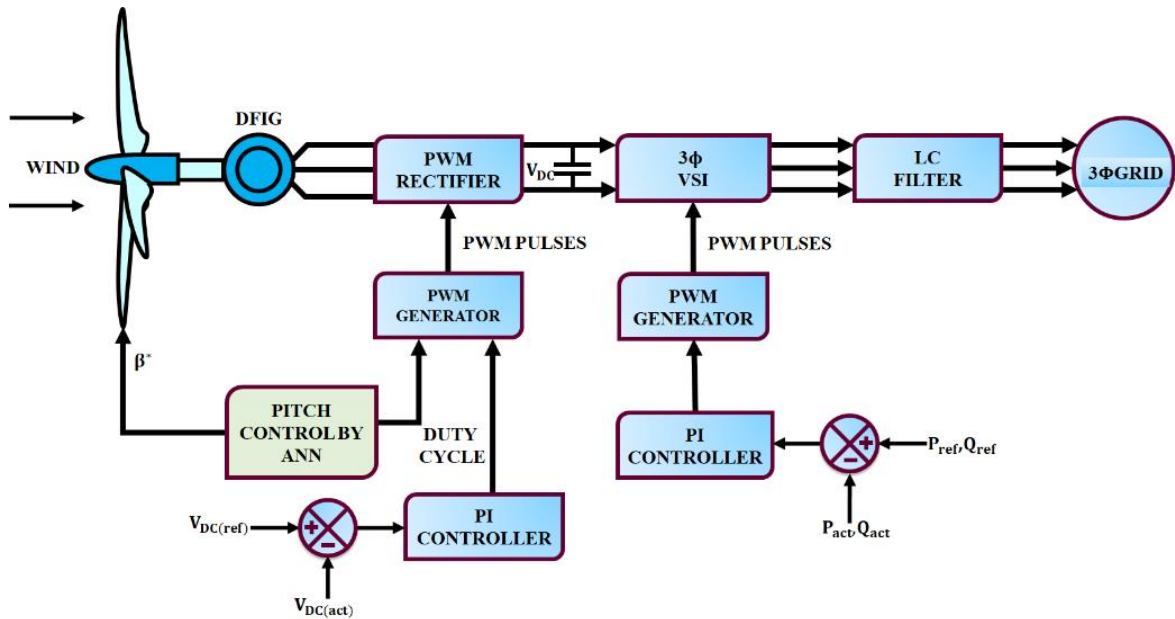


Fig. 1. DFIG-Based WECS.

operation in a range of wind situations. Nevertheless, PID controls struggle to adjust to shifting external circumstances or system dynamics without manual retuning.

The simple optimum intelligent (SOI-PID) controller offers a quick response in numerous functional circumstances. It is better to develop a pitch system and ensure the stability of output power in WT. But, it has poor performance and complexity in managing numerous variables and non-linearity [21]. To allow the servo motor to vary the pitch angle by the preferred value, the P-PI controller provides the reference pitch signal. However, it is complex to predict the optimal values due to the non-linearity [22]. The pitch controller based on LSTM balance for delay since it derives the blade pitch control angle by finding the delay occurrence in the actuator. It has similar performance during changes in wind speed. Nevertheless, the improper selection led to oscillation and slow convergence [23]. The conventional controller needs retuning to function over distinct operating points, which is less efficient. Also, controllers are less reliable and have unstable performance in varying conditions. To overcome the above-mentioned issues, this research develops an ANN controller-based pitch control approach. An ANN controller has the capacity to adapt and learn from data and continuously adjust its weights to sustain optimal parameters and also provide better robustness to varying conditions. The main objectives are,

- The ANN controller is integrated for regulation of turbine blade pitch angles, enhancing energy efficiency and optimizing electricity generation in response to varying wind speeds.
- For assuring compatibility with grid necessities, the

PWM rectifier is exploited to convert variable-frequency AC output from the DFIG to DC power.

- For grid synchronization, improving the compatibility and stability of the power system, a Voltage Source Inverter (VSI) is utilized to convert the DC power back to AC power.
- For enabling steady voltage levels and efficient grid synchronization, the PI controller is employed to align actual and reference power values.

2- Proposed System Methodology

Fig. 1 depicts the novel DFIG-based WECS with an ANN controller to optimize energy conversion and ensure efficient grid integration. The AC supply from DFIG is provided to the PWM rectifier, which converts AC into a DC supply. The ANN controller effectively manages the wind turbine pitch through real-time blade angle changes. The DC power is delivered to a three-phase VSI to convert it into AC power. Then, the PI controller is exploited for maintaining a steady DC link voltage and assures precise grid synchronization by matching the actual power values with the reference values. Furthermore, the LC filter is employed to avert harmonic distortion that enhances the output power quality.

To maximize energy capture and minimize mechanical loads, an ANN-based controller governs the turbine blade pitch angle. The PWM generator supports the rectifier and inverter by generating precise switching pulses to assure effective operation under varying conditions. To maintain operational stability and optimize energy conversion, the control system integrates feedback loops at multiple levels. It not only improves dynamic performance but also enhances

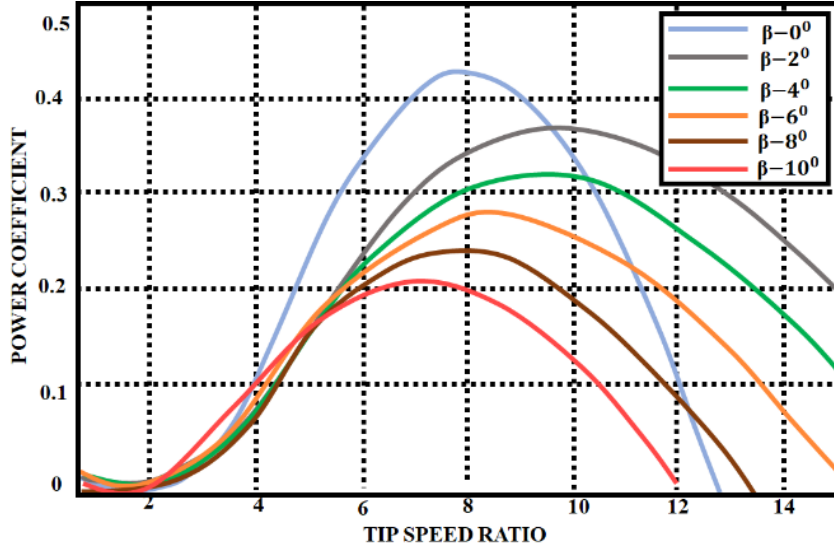


Fig. 2. Power Coefficient Curve.

resilience against disturbances, ensuring reliable and efficient grid integration.

2- 1- DFIG-based WECS

DFIG transforms the kinetic energy of moving air into mechanical energy that is delivered to DFIG, where it is transmuted into electrical power for grid integration or local use. The expression (1) is used for determining mechanical power,

$$P_m = 0.5\rho AC_p(\lambda, \beta)V_{wind}^3 \quad (1)$$

Where air density is ρ , the area swept out by the turbine blade is A , wind speed is v_{wind} and the power coefficient is $C_p(\lambda, \beta)$. It is dependent on two variables The blade pitch angle is β and tip speed ratio is λ .

$$\lambda = \frac{\Omega R}{v_{wind}} \quad (2)$$

Where the radius of the blade is R and angular speed is Ω .

$$C_p(\lambda, \beta) = C_1 \left(\frac{C_2}{\lambda_i} - C_3\beta - C_4 \right) \exp\left(\frac{-C_5}{\lambda_i} \right) + C_6\lambda \quad (3)$$

Where,

$$\frac{1}{\lambda_i} = \left(\frac{1}{\lambda + 0.08\beta} - \frac{0.035}{\beta^3 + 1} \right) \quad (4)$$

The power coefficient and power characteristics curve of WT are shown in Fig. 2 and Fig. 3. The nonlinear power coefficient is expressed as a function of λ and is based on the aerodynamics of turbine blades. The relationship between transmitted power, rotational speed, and mechanical torque is,

$$T_m = \frac{P_m}{\Omega} \quad (5)$$

The optimal angular speed is expressed as,

$$\Omega_{opt} = \lambda_{opt} v_{wind} / R \quad (6)$$

The maximum mechanical power is,

$$P_{m_max} = 0.5\rho AC_{pmax} v_{wind}^3 \quad (7)$$

An asynchronous generator with a wound rotor is called a DFIG. While the rotor is connected via the converter, the stator and grid are connected directly. The DFIG dynamic model represented in an arbitrary rotating frame is simplified by using the following formula:

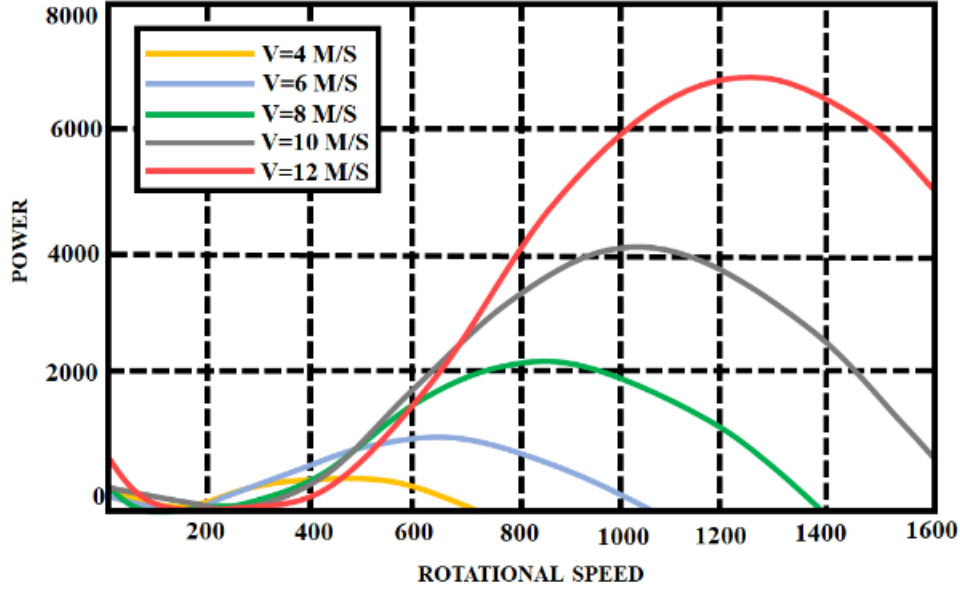


Fig. 3. Wind Turbine Power Characteristics Curve

$$I_{ds}R_s + \frac{d}{dt} \varphi_{ds} - \varphi_{qs} \omega_s = V_{ds} \quad (8)$$

$$I_{qs}R_s + \frac{d}{dt} \varphi_{qs} + \varphi_{ds} \omega_s = V_{qs} \quad (9)$$

$$I_{ds}R_r + \frac{d}{dt} \varphi_{dr} - \varphi_{qs} (\omega_s - \omega_r) = V_{dr} \quad (10)$$

$$I_{qs}R_r + \frac{d}{dt} \varphi_{qr} - \varphi_{ds} (\omega_s - \omega_r) = V_{qr} \quad (11)$$

The synchronous reference frame is represented by d and q , whereas the stator and rotor indices are specified using s and r . Resistance is denoted by R , while electrical frequency, flux, current, and voltage are represented by the symbols ω, φ, I and V , respectively. The flux is defined as,

$$I_{ds}L_s + I_{dr}M = \varphi_{ds} \quad (12)$$

$$I_{qs}L_s + I_{qr}M = \varphi_{qs} \quad (13)$$

$$I_{dr}L_r + I_{ds}M = \varphi_{dr} \quad (14)$$

$$I_{qr}L_r + I_{qs}M = \varphi_{qr} \quad (15)$$

Where, inductance and mutual inductance is indicated by M and L .

The mechanical analysis is,

$$J \frac{d\Omega}{dt} = T_a - T_{em} - f\Omega \quad (16)$$

Where the speed of the generator is Ω , electromagnetic torque is T_{em} and the turbine's total inertia is J . Then, T_{em} becomes,

$$T_{em} = p \frac{M}{L_s} (\phi_{qs} I_{dr} - \phi_{ds} I_{qr}) \quad (17)$$

Grid-side converters and rotor-side converters are two essential parts of a DFIG system that manage the complex process of controlling energy flow between the grid, generator, and load. In order to achieve this, both converters are diligently managed by PI controllers, which are well-known for their dependability and effectiveness in control systems. The difference between the intended and actual system states is continuously evaluated by these PI controllers. They are able to modify the parameters of converters in real time by computing an error signal that represents this discrepancy. Additionally, a PWM rectifier is employed for converting

the DFIG system’s AC output into steady DC power. In order to control the DC output voltage, this rectifier meticulously modifies the width of voltage pulses, guaranteeing a steady and continuous power supply.

2- 2- Pitch control by ANN controller

One efficient way to control or limit turbine performance in high wind speeds is to modify the blades’ pitch angle. Pitch servos, which are electrical or hydraulic systems, are used to move the blades into the required positions. Blade pitch modifications with rotational speeds of roughly 5–10°/s are anticipated during typical operation. In this case, a pitch rate of 8°/s is selected to prevent excessive loads during standard regulating processes. Pitch control, either active or passive, is utilized to safeguard the mechanical and electronic systems and capture as much energy as feasible. Pitch, speed, acceleration, and deceleration are managed to lessen the electrical current peaks and the mechanical tensions in the bucket, tower, and blades.

2- 3- Passive control of pitch

The wings’ angle of attack against the wind is fixed, and the blades are fastened to the hub. When wind speed surpasses a rated value, the rotor’s aerodynamic design loses efficiency.

2- 4- Active control of pitch

When the output power is too high or too small, the blades spin to vary the angle of attack with the wind. To retain a consistent power output, the blades must be able to shift by a fraction of a degree at a time, which corresponds to an alteration in wind speed. The active pitch control system functions in a particular range of wind speeds. This research

uses active pitch control for regulating the pitch of WT. The various control loops of WT are provided in Fig. 4. The four areas of operation are depicted in Fig. 5. Region I denotes wind speeds below the minimum needed to initiate rotation, at which no power is produced. When this speed is surpassed, the rotor begins to rotate and moves into region II, where the generator rotates at its normal speed and is enclosed by the starting and cutting speeds. The third area covers the nominal speed to the stoppage speed, or the maximum speed at which rotation is necessary for safety and design. Lastly, the IV region, where a mechanical brake is required for the wind turbine assembly’s safety. A feedback control system’s objective is to lower the error $e(k)$ among any variable and its set to zero.

The error is calculated as,

$$e(t) = \omega_{ref} - \omega_{rotor}(t) \tag{18}$$

The first-order delay system, or an integrator, is a pitch actuator with a time constant τ_c , which is estimated as,

$$\frac{d\beta}{dt} = -\frac{1}{\tau_c} \beta + 1 \frac{1}{\tau_c} \beta_{ref} \tag{19}$$

Where, maximum and minimum pitch angles are indicated by β_{max} and β_{min} , $\left(\frac{d\beta}{dt}\right)_{min} \leq \frac{d\beta}{dt} \leq \left(\frac{d\beta}{dt}\right)_{max}$ and $\beta_{min} \leq \beta \leq \beta_{max}$.

ANN is utilized in this study to achieve nonlinear, time-varying input-output mapping, enabling effective control

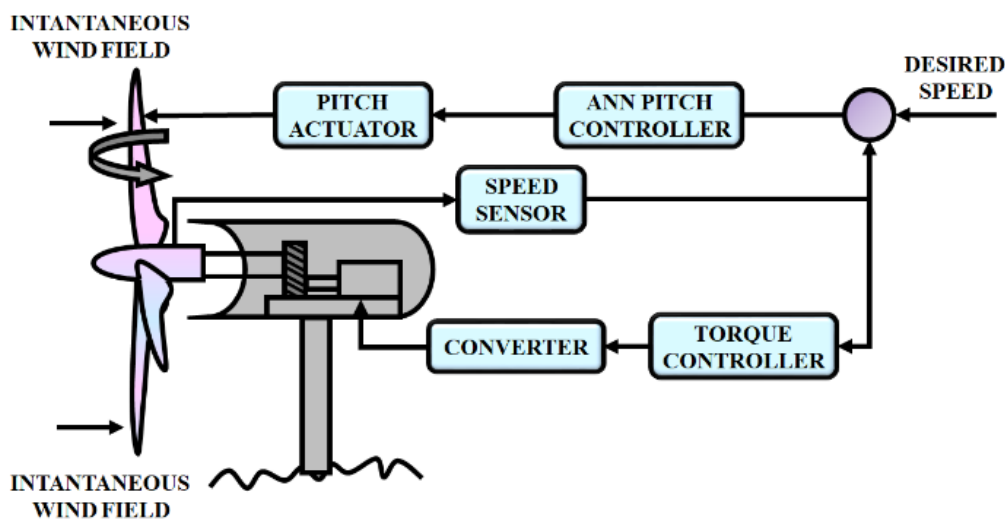


Fig. 4. WT’s Standard Control Loops

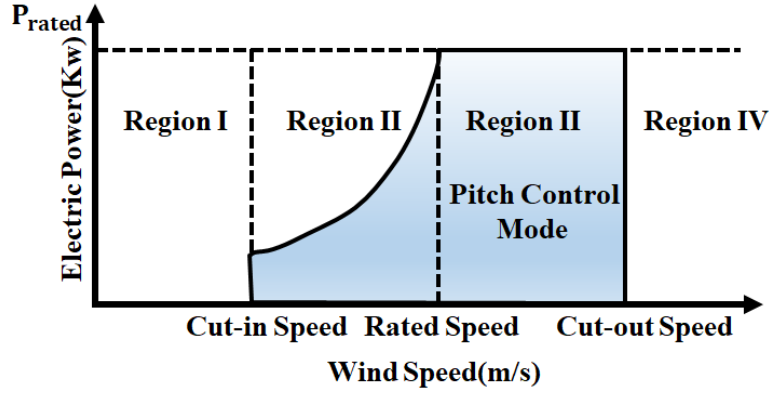


Fig. 5. Wind Turbine Operating Regions.

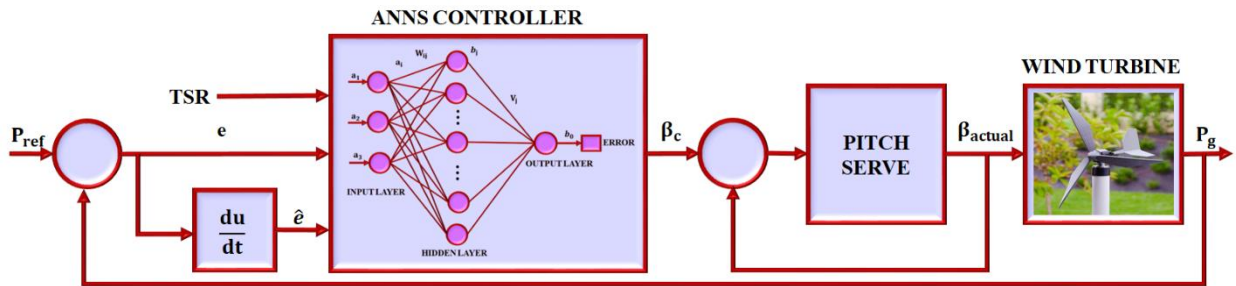


Fig. 6. Structure of ANN Base Pitch Controller.

of the pitch angle in a wind energy system. Wind turbine generating systems exhibit highly nonlinear dynamics, as discussed earlier, making ANN an appropriate choice for pitch regulation. The control method leverages the inverse relationship between the pitch angle and other variables, such as electric power, to serve as the foundation of the developed controller.

$$\hat{\beta} = h^{-1}(\hat{v}, w, P_e) \tag{20}$$

Sensors measure the generating power P_e and rotating speed w_m , while wind speed models forecast wind speed v . The set of wind speed values and the set of pitch angles' historical values are used to determine the control input, which is denoted as

$$BIC(p, q) = \chi^2 + k \cdot \ln(n) \tag{21}$$

The Bayesian Information Criterion (BIC) uses p and q to signify the autoregressive orders and moving average processes, while k denotes the number of parameters in

the statistical model. Predicted wind speed is exploited to determine the desired rotor speed, and historical data, including pitch angles, rotor speed, and real power output, are input into the ANN controller.

The input, hidden, and output layers are the layers presented in the ANN controller. The number of neurons in the hidden layers is 10 to 40, and the input layer has 3 inputs. The transfer function is obtained by the tangent sigmoid function as,

$$\vec{f}_1 = \frac{2}{(1 + e^{-2x_j})} - 1 \tag{22}$$

The output layer's transfer function is obtained by using the sigmoid function as,

$$\vec{f}_2 = \frac{2}{(1 + e^{-x_0})} \tag{23}$$

The output of neuron y is,

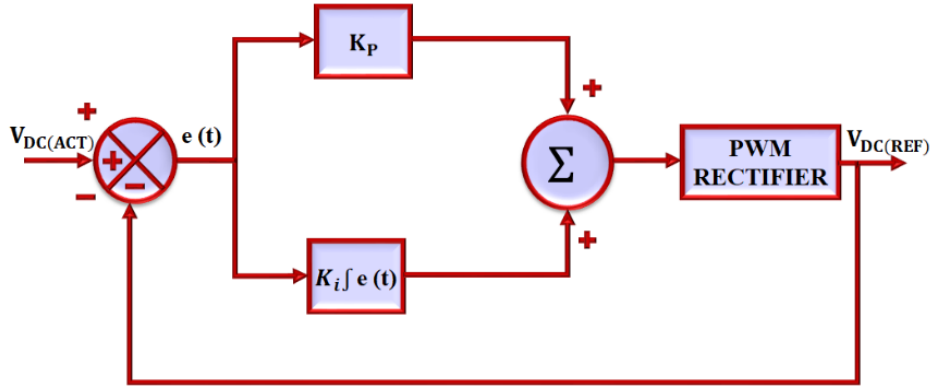


Fig. 7. Structure of PI Controller.

$$y = \vec{f}_2 \left(\vec{v}_j \vec{f}_1 \left(w_{ij} \vec{a}_i + \vec{b}_j \right) + \vec{b}_o \right) \quad (24)$$

The ANN is trained offline using a dataset that covers the entire operational range of the WTDFIG system, as depicted in Fig.6. In this system, sensors identify the sample point of \hat{P}_e and w_m and the wind speed ARMA model provides the \hat{v} .

2- 5- PI CONTROLLER

A PI controller comprises the control error based on settling value and process output and makes output according to the error's proportion and integral, as revealed in Fig.7. The control signal is,

$$K_p e(t) + K_i \int_0^t e(t) dt + u_0 = u(t) \quad (25)$$

Where the integral parameter is K_i , The initial output is u_0 and the proportion parameter is K_p . The error at time t is,

$$y_{sp}(t) - y(t) = e(t) \quad (26)$$

Where the set point is $y_{sp}(t)$ and the process output is $y(t)$. The transfer function of the PI controller is,

$$G_c(s) = \frac{U(s)}{E(s)} = K_p + \frac{K_i}{s} \quad (27)$$

3- Result and Discussions

The proposed system introduces DFIG-based WECS integrated with advanced control strategies to optimize energy conversion and ensure efficient grid integration. For

maximum power extraction under varying wind conditions, reducing mechanical stress, an ANN-based pitch controller dynamically adjusts turbine blade angles. The MATLAB/Simulink simulations reveal the system's performance based on the parameters denoted in Tables 1 and 2.

Fig. 8(a) reveals that the wind speed is stable at 15 m/s. For a reliable analysis and control process by maintaining stable aerodynamic input to the wind turbine, this steady wind speed provides a uniform operating condition. Fig. 8(b) has fluctuations within the range of -1.3 Nm to -0.7 Nm.

Fig. 9 offers the various operational characteristics of DFIG during energy conversion. The rotor speed is settled at 1.25 rad/s, which denotes the stable operation of the rotor under given conditions. The waveform of the voltage indicates a balanced and stable voltage generation. The current waveform has stable amplitude and frequency.

Fig. 10 represents the pitch angle of DFIG with minor fluctuations observed in the early stage. It reveals that the dynamic adjustments by the control system in response to variations in system requirements. The improvement in pitch angle denotes the ANN controller optimizing the blade angles to sustain efficient energy extraction and alleviate mechanical stress on WT.

The behaviour of the DC link voltage is depicted in Fig. 11, which stabilizes at 600V. It assures efficient energy conversion and compatibility with grid necessities. Fig. 12 illustrates the behaviour of grid parameters when integrated with WECS. The voltage and current are stable. An efficient power transfer with minimal reactive power is offered by the alignment of voltage and current in phase.

The waveforms of real and reactive power are represented in Fig. 13. It denotes that the system effectively manages both real and reactive power under steady conditions. It reveals the development of a control approach to optimize power generation and sustain the stability of the grid.

The waveforms of THD are displayed in Fig. 14. The R, Y, and B phases maintain values of 0.90%, 0.65%, and 0.93%, indicating better power quality.

The ANN controller attains the most stable output power

Table 1. WECS's Parameter Specifications.

Parameters	Values	Parameters	Values
Nominal power	10kW	Line voltage	415V
Frequency	50Hz	Gear ratio	100
Turbines	4	Tip speed ratio	7
Power coefficient	0.4421	Pole pair	2

Table 2. ANN Controller's Parameter Specifications.

Parameters	Values	Parameters	Values
Activation function	ReLU	Hidden layers	3
Neurons per layer	15	Learning rate	0.005
Training algorithm	Adam optimizer	Sampling time	0.5s
Pitch actuation time	8° / s	Momentum parameter	0.9
Maximum iteration	200 epochs	Error threshold	0.0001

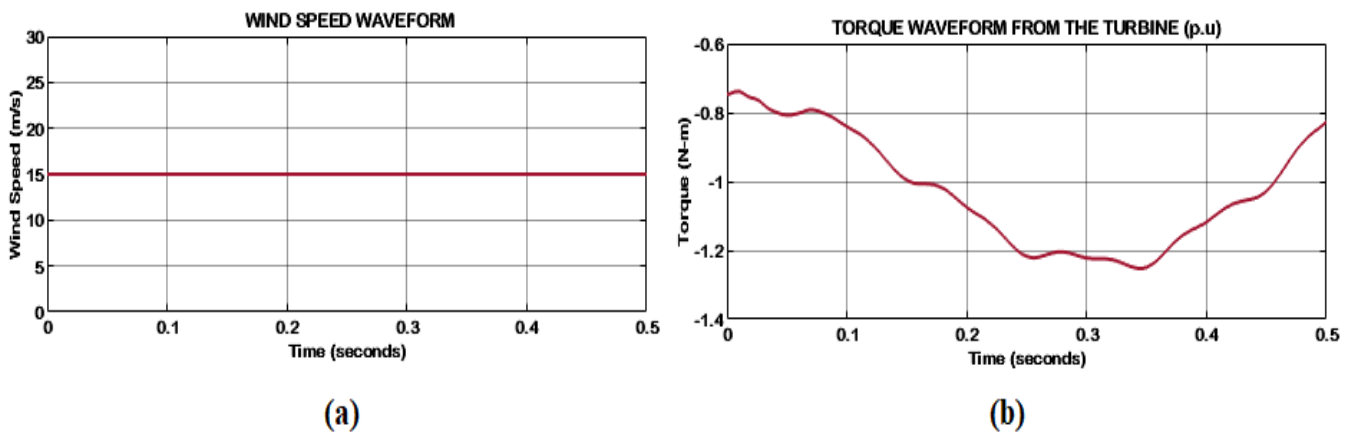


Fig. 8. Waveforms of (a) Wind speed and (b) Wind turbine torque.

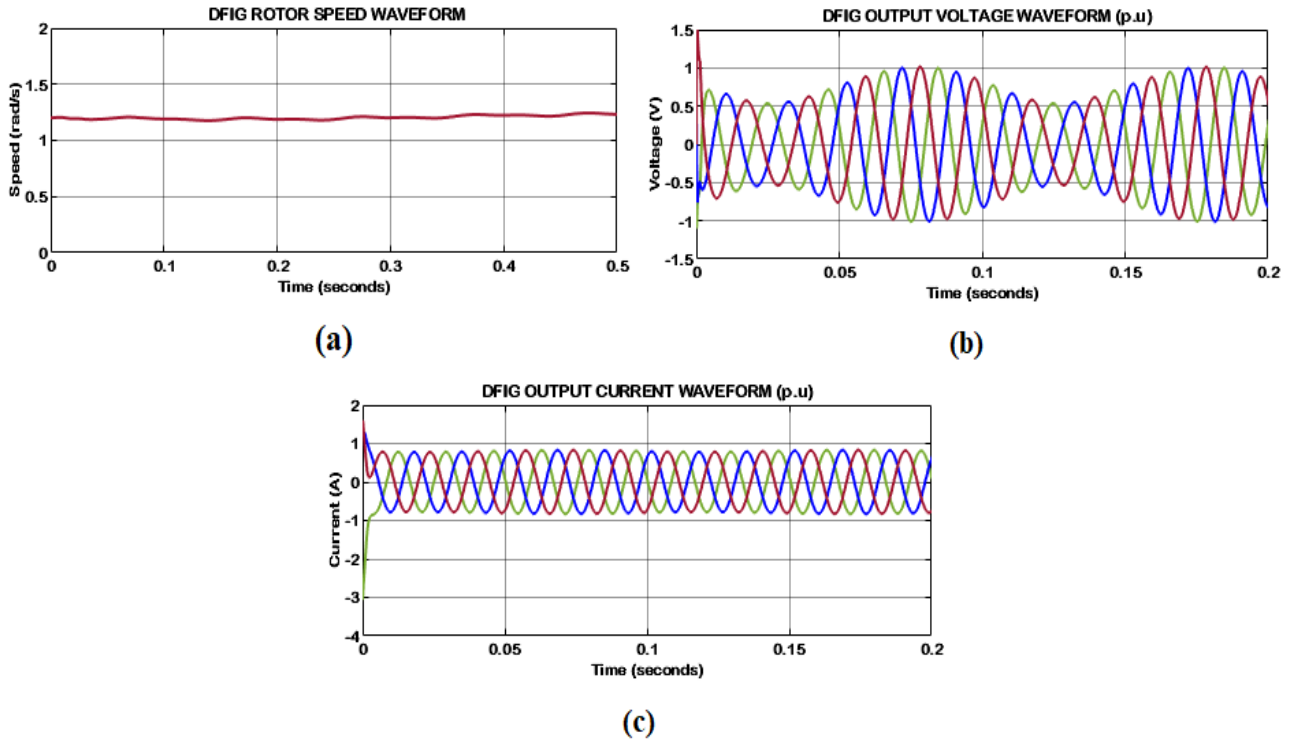


Fig. 9. Waveforms of DFIG for (a) Rotor Speed, (b) Output Voltage, and (c) Current.

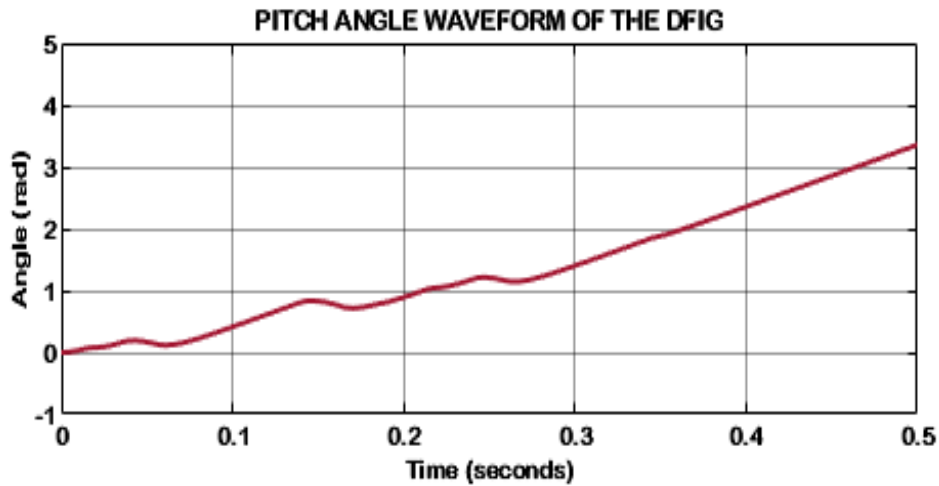


Fig. 10. Pitch Angle of DFIG

with minimal torque fluctuations, as denoted in Table 3. Also, it provides the quickest settling time and reduced overshoot assures a precise response to changes. The ANN controller is computationally efficient and highly adaptable, with a maximum simulation time efficiency compared to PI and PID controllers.

3- 1- Assessment of the developed work under turbulent intensity

Fig. 15 depicts an evaluation of the frequency domain, which denotes that the ANN controller outperforms the PI controller in alleviating Blade-Root Bending Moments (BRBMs) at a wind speed of 16 m/s. The PI controller has

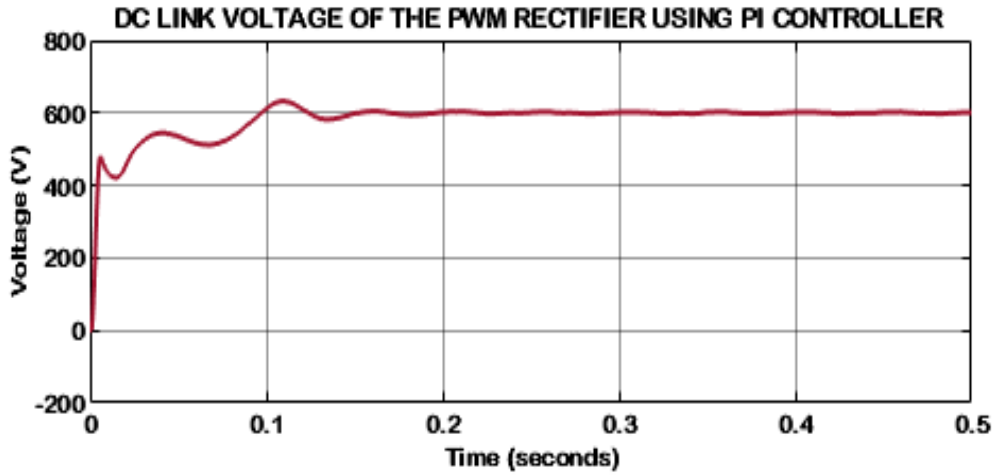


Fig. 11. DC Link Voltage Waveform.

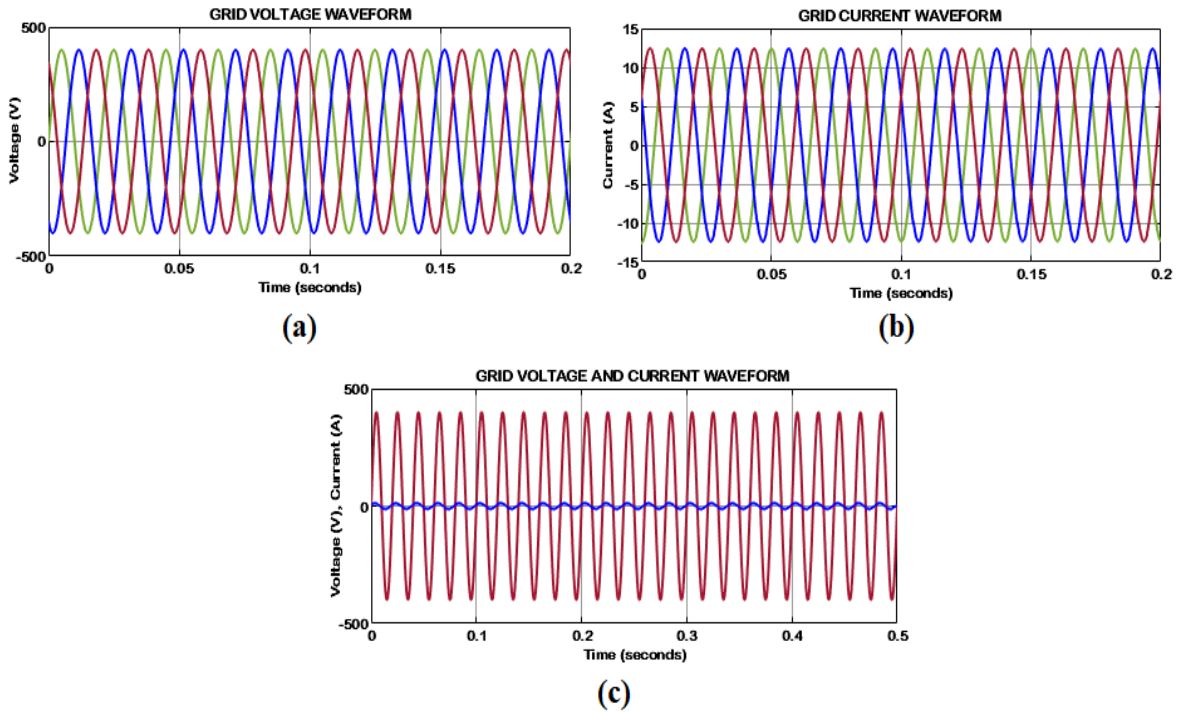


Fig. 12. Waveforms of Grid for (a) Voltage (b) Current, and (c) Single Phase.

maximum magnitude and superior phase lag, predominantly in the low-frequency range, representing reduced effectiveness in handling high and dynamic -frequency loads. Thus, the ANN controller attains small magnitudes over the frequency, proving better load suppression and adaptability.

The response of wind turbines to an Extreme Operating Gust (EOG) at a wind speed of 16 m/s with turbulent intensity

is depicted in Fig. 16. There is a sharp spike between 40 and 50 s; at this period, the BRBMs experience significant fluctuations. The Ann controller has better performance by reducing BRBM peaks and ensuring smoother recovery post-gust, emphasising its adaptability. The lower efficiency in mitigating extreme loads is indicated by a PI controller that has the highest BRBM magnitudes. Fig. 17 reveals the

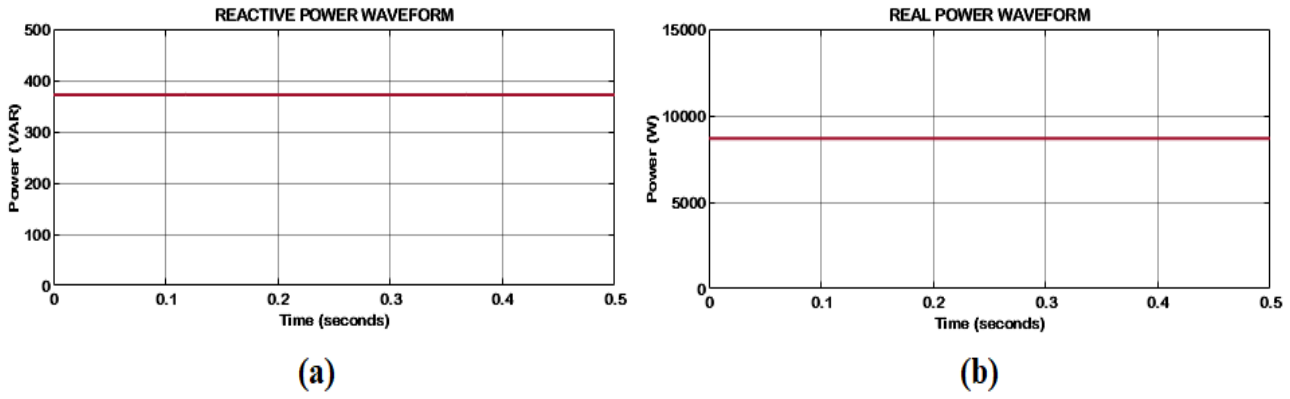


Fig. 13. Waveforms of Real and Reactive Power.

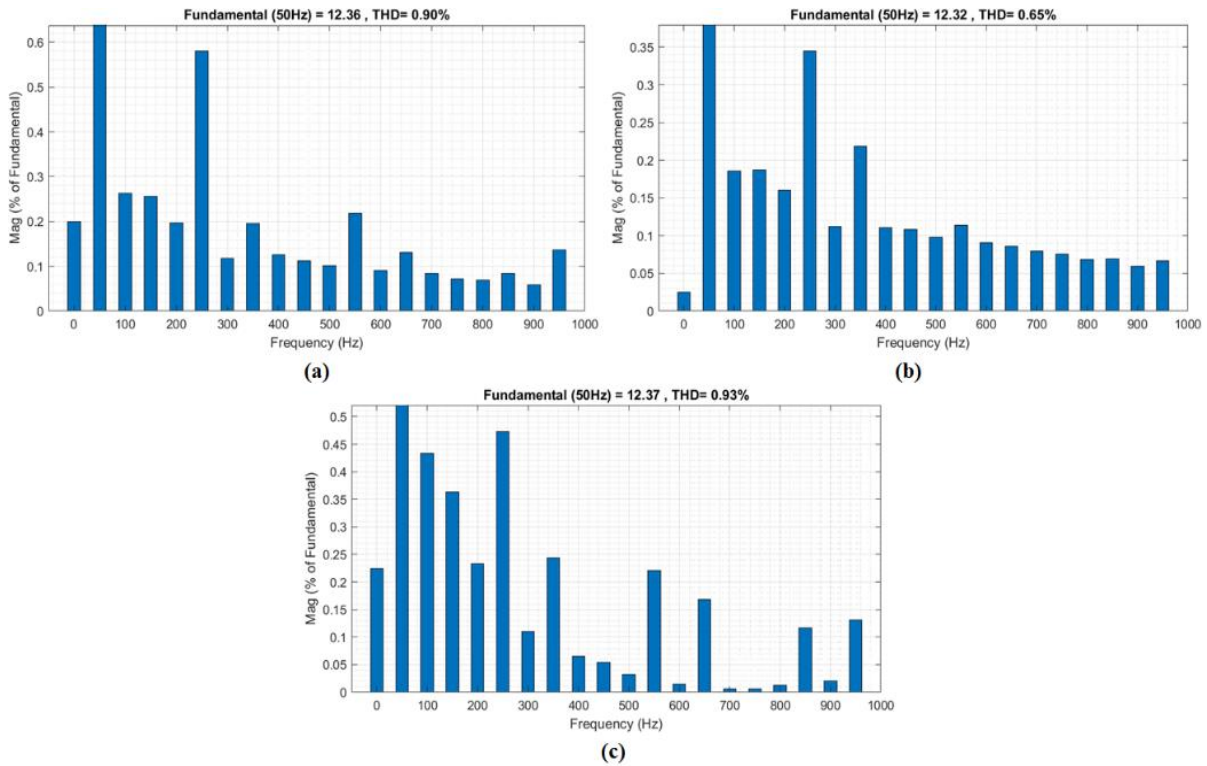


Fig. 14. THD Waveforms.

response of EOG at a wind speed of 14m/s with turbulent intensity. The ANN controller manages transient aerodynamic conditions, assures operational stability, and structural safety.

The responses of PI, PID, and ANN controllers during EOG at 14 m/s wind speed is shown in Fig. 18. The PI controller has oscillations and sluggish recovery in power output and generator speed, representing poor performance

under gust conditions. The ANN controller has superior performance, sustaining minimal deviations and consistent power regulation. Fig. 19 displays the response of generator speed and power output to EOG at a wind speed of 16 m/s. Here, the ANN controller has the best performance by sustaining reduced deviations and smooth recovery.

The effectiveness of PI, PID, and ANN controllers is

Table 3. Performance Evaluation of Controllers for Pitch Angle Regulation.

Parameter	PI controller	PID controller	ANN controller
Output power stability (W)	10,000 ± 25	10,000 ± 15	10,000 ± 5
Torque fluctuations (Nm)	±0.4	±0.25	±0.1
Settling time (s)	0.35	0.25	0.15
Overshoot (%)	10%	6%	2%
Mechanical stress (kNm)	85	70	50
Pitch Actuation Rate (°/s)	12	10	8
Simulation time efficiency	85%	90%	95%

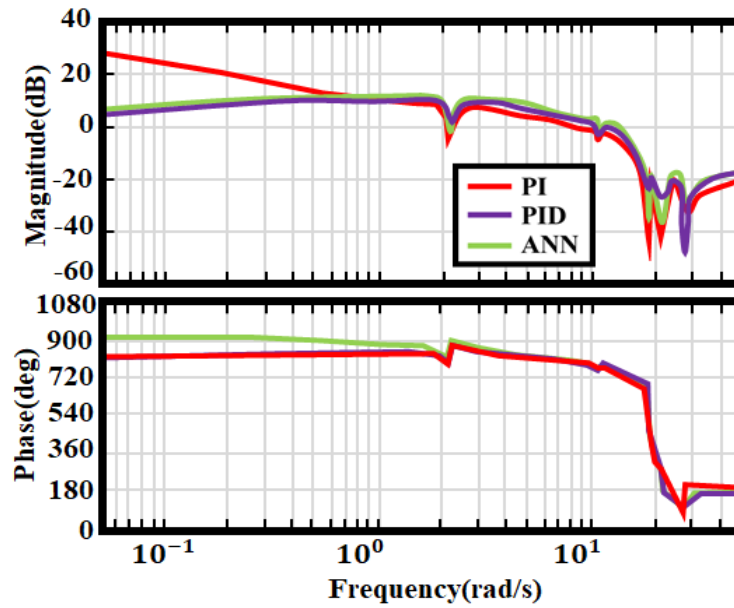


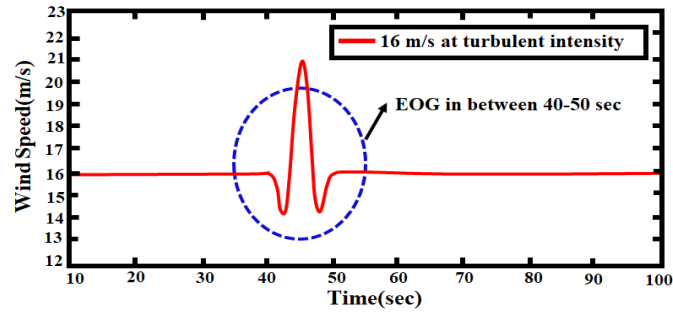
Fig. 15. Evaluation of Frequency Domain.

depicted in Table 4. The PI controller has the highest standard deviation, while the PID controller has reduced standard deviations to 0.0786 at 14 m/s. But the ANN controller minimizes generator speed fluctuations and sustains stability under turbulent conditions.

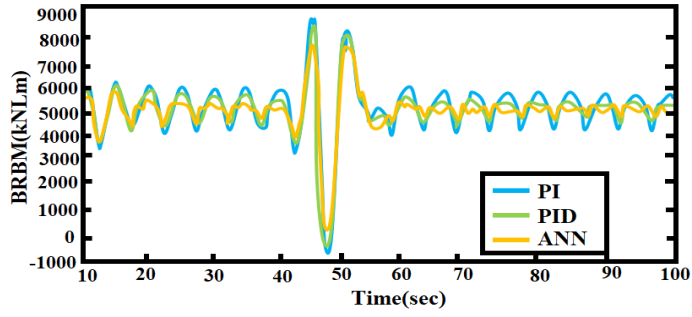
The performance of PI, PID, and ANN controllers is displayed in Table 5. The ANN controller steadily outperforms the others, attaining the lowest standard deviations of 1.184×10^3 kNm at 14 m/s and 1.287×10^3 kNm at 16 m/s, representing superior stability and load reduction for tilt moment. The

ANN controller attains better performance with deviations to 1.123×10^3 kNm at 14 m/s and 1.255×10^3 kNm at 16 m/s in yaw moments. It demonstrates that the ANN controller's superior ability to manage dynamic loads and sustain system stability under turbulence.

The performance analysis of controllers with Mean Squared Error (MSE) and Root Mean Squared Error (RMSE) is revealed in Table 6. The proposed approach has the lowest MSE and RMSE of 0.00013 and 0.0254, indicating the overall performance of the system is enhanced.

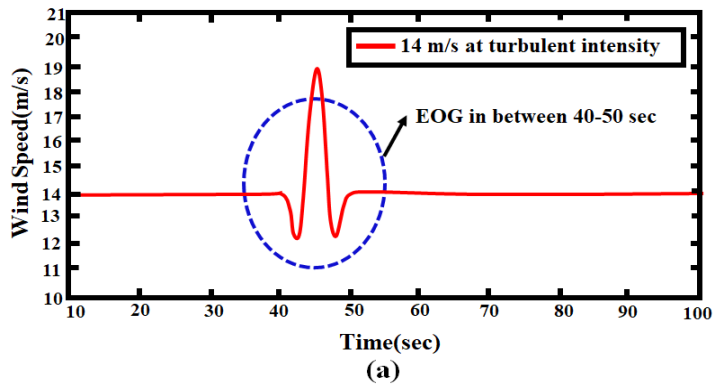


(a)

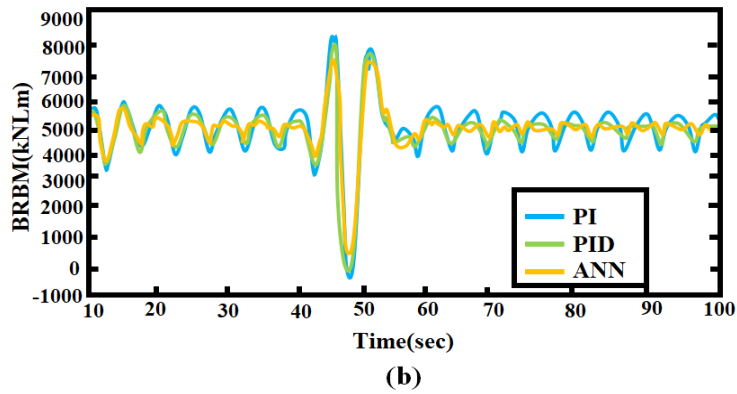


(b)

Fig. 16. Wind Speed and Blade-Root Bending Moments at 16 M/S and Turbulent Intensity.



(a)



(b)

Fig. 17. Wind Speed and Blade-Root Bending Moments at 14 M/S and Turbulent Intensity.

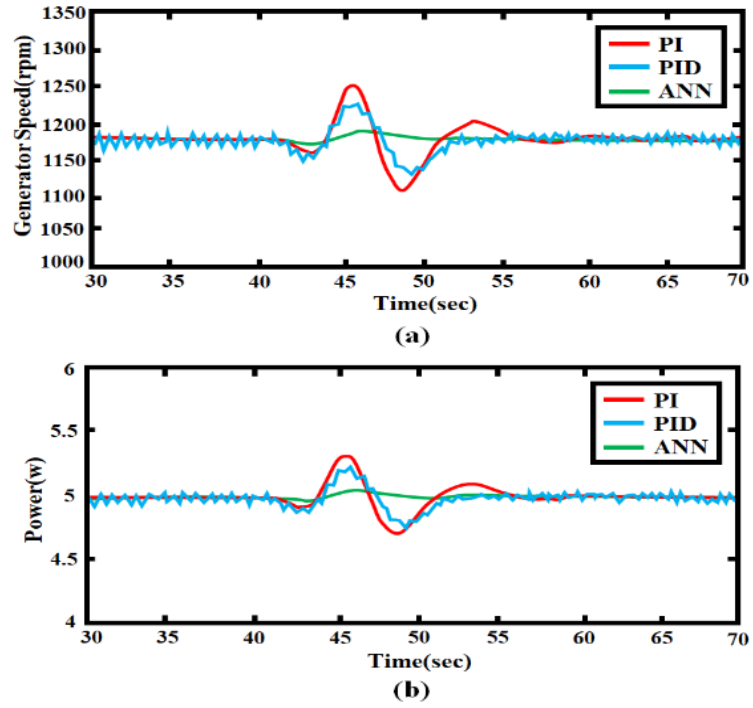


Fig. 18. Dynamic Response and Power Output to EOG at 14 M/S Wind Speed.

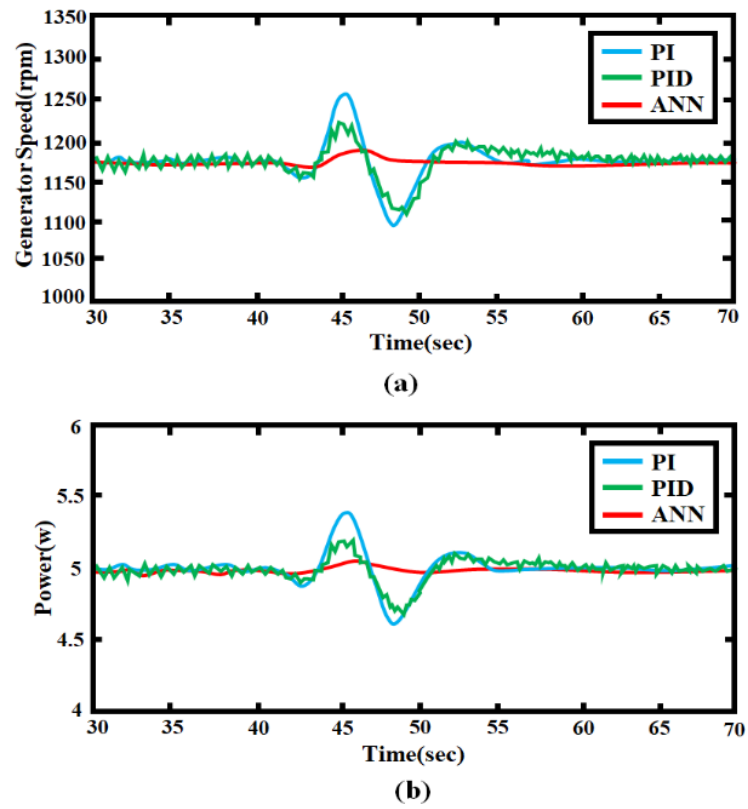


Fig. 19. Dynamic Response and Power Output to EOG at 16 M/S Wind Speed.

Table 4. Efficacy Evaluation of Controllers.

Parameters	PI controller		PID controller		ANN controller	
	14 m/s	16 m/s	14 m/s	16 m/s	14 m/s	16 m/s
Standard deviation	0.1815	0.1835	0.0786	0.0824	0.0205	0.0208
% reduction	-	-	56.74%	55.10%	88.70%	88.65%

Table 5. Controller Performance in Managing Tilt and Yaw Moment Fluctuations under Turbulence.

Standard Deviation (kNm)	Controller	At Wind Speed (14 m/s)		At Wind Speed (16 m/s)	
Tilt moment	PI controller	1.265×10^3		1.428×10^3	
	PID controller	1.238×10^3		1.372×10^3	
	ANN controller	1.184×10^3		1.287×10^3	
Yaw moment	PI controller	1.202×10^3		1.386×10^3	
	PID controller	1.171×10^3		1.370×10^3	
	ANN controller	1.123×10^3		1.255×10^3	

Table 6. Performance Analysis of Controllers.

Approaches	MSE	RMSE
PID	1.296E-7	0.00036
RNN	3.28E-11	5.54E-06
Proposed	0.00013	0.0254

Table 7. Analysis of THD.

Approaches	THD
FOSMC	1.38%
SOSMC	1.28%
TOSMC	1.06%
Proposed	0.65%

Table 7 displays the analysis of THD for FOSMC, SOSMC, TOSMC, and the proposed approach, which has the lowest THD of 0.65% among others, denoting that the power quality is enhanced, maximizing power generation.

4- Conclusion

A novel pitch control technique based on an ANN for enhancing the efficiency of wind energy systems is developed in this research. By dynamically regulating the blade pitch to optimal angles, the ANN aids in enhancing the efficacy of energy conversion from wind to electrical power, safeguarding reliable and stable operation. The AC voltage from wind turbines is transformed into DC voltage by a PWM rectifier, regulate the magnitude of the output voltage. The DC power produced by the PWM rectifier is given to an inverter that transforms it into AC power, guaranteeing that the power from the wind turbine is well-suited with the electrical grid. Moreover, the output achieved is transformed into AC using 3ϕ VSI and by achieving grid synchronization with the help of a PI controller, the DC link voltage is delivered to the grid. The results have been applied in MATLAB/ Simulink, proving that the developed work provides better performance. Simulation results validate the superior performance of the ANN controller over conventional PI and PID controllers, demonstrating reduced generator speed fluctuations, lower mechanical stress, and enhanced power stability. The ANN controller has minimal overshoot, quicker response times, and better dynamic stability under extreme wind events. Nevertheless, tuning of the ANN controller is more complex and intensive, needs more sophisticated hardware for real-world applications.

References

- [1] S. Al-Janabi, A. F. Alkaim, and Z. Adel, "An Innovative synthesis of deep learning techniques (DCapsNet & DCOM) for generation of electrical renewable energy from wind energy", 2020 *Soft Computing*, vol. 24, no. 14, pp. 10943-10962.
- [2] W. S. Udo, J. M. Kwakye, D. E. Ekechukwu, and O. B. Ogundipe, "Optimizing wind energy systems using machine learning for predictive maintenance and efficiency enhancement", 2024 *Journal of Renewable Energy Technology*, vol. 28, no. 3, pp. 312-330.
- [3] R. Gianto, "Steady-state model of DFIG-based wind power plant for load flow analysis", 2021 *IET Renewable Power Generation*, vol. 15, no. 8, pp. 1724-1735.
- [4] N. A. Dwijendra, T. J. Abduladheem, A. M. B. S. Abed, Bashar, A. J. Al-Nussairi, A. T. Hammid, A. Shamel, and K. F. Uktamov, "Improving the transition capability of the low-voltage wind turbine in the sub-synchronous state using a fuzzy controller", 2022 *Clean Energy*, vol. 6, no. 4, pp. 682-692.
- [5] S. Sarkar, B. Fitzgerald, and B. Basu, "Individual blade pitch control of floating offshore wind turbines for load mitigation and power regulation", 2020 *IEEE Transactions on Control Systems Technology*, vol. 29, no. 1, pp. 305-315.
- [6] H. Ren, B. Hou, G. Zhou, L. Shen, C. Wei, and Q. Li, "Variable pitch active disturbance rejection control of wind turbines based on BP neural network PID", 2020 *IEEE Access*, vol. 8, pp. 71782-71797.
- [7] M. Elsisi, M. Q. Tran, K. Mahmoud, M. Lehtonen, and M. F. Darwish, "Robust design of ANFIS-based blade pitch controller for wind energy conversion systems against wind speed fluctuations", 2021 *IEEE Access*, vol. 9, pp. 37894-37904.
- [8] H. Badihi, Y. Zhang, P. Pillay, and S. Rakheja, "Fault-tolerant individual pitch control for load mitigation in wind turbines with actuator faults", 2020 *IEEE Transactions on Industrial Electronics*, vol. 68, no. 1, pp. 532-543.
- [9] D. Bustan, and H. Moodi, "Adaptive interval type-2 fuzzy controller for variable-speed wind turbine", 2020 *Journal of Modern Power Systems and Clean Energy*, vol. 10, no. 2, pp. 524-530.
- [10] C. Zhang, and F. Plestan, "Individual/collective blade pitch control of floating wind turbine based on adaptive second order sliding mode", 2021 *Ocean Engineering*, vol. 228, pp. 108897.
- [11] J. E. Sierra-García, and S. Matilde, "Improving wind turbine pitch control by effective wind neuro-estimators", 2021 *IEEE Access*, vol. 9, pp. 10413-10425.
- [12] V. L. Narayanan, and R. Ramakrishnan, "Design and implementation of an intelligent digital pitch controller for digital hydraulic pitch system hardware-in-the-loop simulator of wind turbine", 2021 *International Journal of Green Energy*, vol. 18, no. 1, pp. 17-36.
- [13] Z., Lin, and X. Liu, "Wind power forecasting of an offshore wind turbine based on high-frequency SCADA data and deep learning neural network", 2020 *Energy*, vol. 201, pp. 117693.
- [14] P. Korkos, M. Linjama, J. Kleemola, and A. Lehtovaara, "Data annotation and feature extraction in fault detection in a wind turbine hydraulic pitch system", 2022 *Renewable Energy*, vol. 185, pp. 692-703.
- [15] P. Chen, D. Han, F. Tan, and J. Wang, "Reinforcement-based robust variable pitch control of wind turbines", 2020 *IEEE Access*, vol. 8, pp. 20493-20502.
- [16] M. Lara, J. Garrido, M. L. Ruz, and F. Vázquez, "Adaptive pitch controller of a large-scale wind turbine using multi-objective optimization", 2021 *Applied Sciences*, vol. 11, no. 6, pp. 2844.
- [17] A. Fekih, S. Mobayen, and C. C. Chen, "Adaptive robust fault-tolerant control design for wind turbines subject to pitch actuator faults", 2021 *Energies*, vol. 14, no. 6, pp. 1791.
- [18] C. Zhang, and F. Plestan, "Adaptive sliding mode control of floating offshore wind turbine equipped by permanent magnet synchronous generator", 2021 *Wind Energy*, vol. 24, no. 7, pp. 754-769.

- [19] Q. Hawari, T. Kim, C. Ward, and J. Fleming, "A robust gain scheduling method for a PI collective pitch controller of multi-MW onshore wind turbines", 2022 Renewable Energy, vol. 192, pp. 443-455.
- [20] J. E. Sierra-Garcia, M. Santos, and R. Pandit, "Wind turbine pitch reinforcement learning control improved by PID regulator and learning observer", 2022 Engineering Applications of Artificial Intelligence, vol. 111, pp. 104769.
- [21] N. M. Mousa, Y. I. El-Shaer, and M. A. El-Sebah, "A proposed controller for pitch angle of wind turbine," 2023 WSEAS Transactions on Systems and Control, vol. 18, pp. 527-539.
- [22] A. Khurshid, M. A. Mughal, A. Othman, T. Al-Hadhrami, H. Kumar, I. K. Arshad, and J. Ahmad, "Optimal pitch angle controller for DFIG-based wind turbine system using computational optimization techniques," 2022 Electronics, vol.11, no. 8, pp. 1290.
- [23] C. Roh, "Deep-learning-based pitch controller for floating offshore wind turbine systems with compensation for delay of hydraulic actuators," 2022 Energies, vol.15, no. 9, pp. 3136.

HOW TO CITE THIS ARTICLE

T. A. Kiran, D. R. Kishore, A. N. Pavani, B. U. Maheswari, Ch. S. Kumari, *Innovative Wind Energy System Featuring ANN-Controlled Pitch Regulation for Efficient Grid Integration*, AUT J. Elec. Eng., 58(3) (2026) 1-588.

DOI: [10.22060/ej.2026.24404.5701](https://doi.org/10.22060/ej.2026.24404.5701)



